Recursive intermediate factorization and complete computational linearization of the coupled-cluster single, double, triple, and quadruple excitation equations*

Stanislaw A. Kucharski and **Rodney J. Bartlett**
Quantum Theory Project, University of Florida, Departments of Chemistry and Physics, Gainesville, FL 32611, USA

Summary. The nonlinear CCSDTQ equations are written in a fully linearized form, via the introduction of computationally convenient intermediates. An efficient formulation of the coupled cluster method is proposed. Due to a recursive method for the calculation of intermediates, all computational steps involve the multiplication of an intermediate with a T vertex. This property makes it possible to express the CC equations exclusively in terms of matrix products which can be directly transformed into a highly vectorized program.

Key words: Coupled cluster equations – Matrix products – Vectorized program

1. Introduction

The main advantage of the coupled cluster (CC) method [1, 2] over the CI approach for electron correlation, relies on the fact that it offers an attractive truncation scheme. It is well known that the full CC method and the full CI approach both provide exact (size)-extensive results. Since neither method in its full expansion is suitable for calculations of real chemical systems, simplifications are requisite. The truncation scheme in the CC approach does not violate extensivity and in addition it generates a method for including higher excitations at much lower cost than in the corresponding CI model.

After applications by Paldus, Čížek, and Shavitt [3], the general *ab initio* application of the CC method to the evaluation of the molecular correlation energy began with an implementation by Bartlett and Purvis [4] and independently by Pople et al. [5] of the CCD model in 1978. From that time the CC method underwent a substantial development. The obvious direction for the improvement of the CCD model was the inclusion of other connected cluster

---

operators. Adding the single excitations defines CCSD, first formulated and implemented by Purvis and Bartlett [6]. Although terms were gathered into natural intermediates, the very large number of terms in CCSD compared to CCD made the coding comparatively difficult.

The inclusion of triple excitation clusters [3] was performed in several stages, starting with the CCSDT-1 method [7], through several intermediate and noniterative CCSD + T(CCSD) steps [8, 9] until ending with the full inclusion of triples which creates the method, CCSDT [10]. The latter method, along with many of its less time consuming approximations [7–9], proved to be able to provide highly accurate correlated results. The next obvious step was to include connected quadruple excitations, i.e. T_4, which has been done at the CCSDTQ-1 [11], CCSDT + Q(CCSDT) [11], and CCSD + TQ*(CCSD) [12] levels, all of which are correct through fifth order.

From the computational point of view, the basic characteristic of each approximation is how the calculation scales with the number of basis functions occupied, n, and excited, N. The CCD method scales as n^2N^4, the inclusion of singles does not change this since the new diagrams require no higher than an n^2N^3 scheme. Inclusion of T_3 clusters increases the scaling factor by 1 or 2 depending upon the types of diagrams included. Those which do not contain the T_3 into T_3 contribution – obtained via the two-body interaction – scale as n^3N^4 and the others as n^3N^5. An analogous situation occurs in the T_4 equation. All the terms which do not include T_4 into T_4 contributions scale as n^4N^5 while the others scale as n^4N^6.

An attractive feature of the CC method is the possibility of diagram factorization [13], i.e., a procedure which allows one to compute a contribution from terms in a piece-wise manner. This feature is intrinsic to CC calculations. It is due to this fact that the CCD method scales computationally as n^2N^4 although the diagrams of quadruple type contain eight lines and when not factorized would require an n^4N^4 scheme. The factorization of diagrams resulting directly from an exponential expansion of the CC wave function is, in fact, the key feature of the CC method. This determines the computational efficiency of a CC program, and provides important advantages compared to analogous CI approaches, in addition to CC methods' extensivity. Obviously both methods tend to converge with the inclusion of higher rank clusters. The lowest order difference between CISD and CCSD results occurs in the fourth-order quadruple contribution, E_4^Q, whereas for CCSDTQ and CISDTQ, the lowest-order corrections neglected by CI are sixth-order pentuples and hextuples. CCSDTQ is correct through sixth order, while CISDTQ is only correct through fifth.

The aim of the present paper is to demonstrate a factorization of all diagrammatic terms occurring in the CCSDTQ method in such a way that the final equations contain only linear terms. This requires suitably defined intermediates, such that all multiple T vertices will be absorbed into them. In addition, the intermediates themselves will be constructed in a recursive manner, i.e., each diagram contributing to the intermediate is also linear in T. It can be observed that the intermediates introduced in the process of factorization of the CC equations are those which appear in the expansion of suitably defined effective hamiltonians. The definition and the diagrammatic expansion of the effective hamiltonian will be briefly discussed in the next section.

2. Effective hamiltonian

When the hamiltonian,

$$H = \sum_{p,q} f_{pq} \{p^\dagger q\} + \tfrac{1}{4} \sum_{p,q,r,s} \langle pq \parallel rs \rangle \{p^\dagger q^\dagger sr\} = F_N + W_N$$

of a system is subjected to a similarity transformation:

$$\tilde{H} = U^{-1} H U \tag{1}$$

the resulting operator $\tilde{H}$ is an effective hamiltonian [14]. The $\tilde{H}$, obtained in Eq. (1), is defined in the full functional space M. Usually the transformation of Eq. (1) is designed in such a way that the eigenvalues of H can be obtained by diagonalizing $\tilde{H}$ in some smaller subspace of M, called a model or active space and defined by a projector P. In this manner we arrive at the more familiar definition of the effective hamiltonian employed in multi-reference theories:

$$H^{\mathit{eff}} = P \tilde{H} P \tag{2}$$

In the present case we are going to use the effective hamiltonian defined in the more general way according to Eq. (1), but with a precisely defined operator U. We assume that U is approximated by the coupled cluster ansatz, i.e., our effective hamiltonian $\bar{H}$ is expressed as:

$$\bar{H} = e^{-T} H e^{T} = (H e^{T})_C \tag{3a}$$

where T is the usual connected cluster operator:

$$T = \sum_{m}^{N} T_m \tag{3b}$$

and

$$T_m = (m!)^{-2} \sum_{\substack{abc\ldots \\ ijk\ldots}} t_{ij\ldots}^{ab\ldots} \{a^\dagger b^\dagger \ldots jki\} \tag{3c}$$

The $\bar{H}$ operator is a quantity of interest for several reasons. Due to the Hausdorff formula, $\bar{H}$ can be expanded in terms of commutators only, which is equivalent to its expansion in terms of connected diagrams as in Eq. (3a). This means that $\bar{H}$ is represented by finite sets of diagrams. Usually the T operator is truncated at a certain level of excitation, and this corresponds to the analogous truncation in the expansion of $\bar{H}$.

The other reason for $\bar{H}$ being worth attention is the fact that it is a quantity that occurs in various computational schemes based upon the cluster expansion of the wave function.

In the treatment of one-electron properties [15, 16] including analytical gradients, the linear response of T amplitudes, T^λ, to a perturbation characterized by λH^λ, is obtained by solving the following equations:

$$\langle \Phi_{ij\ldots}^{ab\ldots} | \bar{H}^\lambda + [\bar{H}, T^\lambda] | \Phi \rangle = 0 \tag{4}$$

where the effective perturbation $\bar{H}^\lambda$ is expressed as:

$$\bar{H}^\lambda = e^{-T} H^\lambda e^{T} \tag{5}$$

In the equation-of-motion approach to the coupled cluster excitation energy [15, 17–19] we arrive at a commutator equation of the form:

$$[\bar{H}, \Omega_k^\dagger] | \Phi \rangle = \omega_k \Omega_k^\dagger | \Phi \rangle \tag{6}$$

where $\Omega^{\dagger}$ is an excitation operator. Again the first step in the solution of Eq. (6) is the construction of the $\bar{H}$ operator [18].

A similar procedure is employed in the multi-reference coupled cluster theory based upon the Fock space ansatz [20–23]. The equation for the n-particle, m-hole sector of Fock space can be generally written as:

$$Q^{(n,m)}(\bar{H}\hat{\Omega} - \hat{\Omega}\bar{H}^{eff})P^{(n,m)} = 0 \tag{7}$$

where $\hat{\Omega}$ is a normal-ordered exponential operator (see [22] for details). Again, the solution of the equation depends on the prior evaluation of $\bar{H}$. In the next sections we are going to analyze the structure of $\bar{H}$ and then describe its recursive construction to demonstrate how the intermediates contributing to $\bar{H}$ can be exploited in the regular coupled cluster equations.

3. Structure of $\bar{H}$

As was already mentioned $\bar{H}$ is expressed in terms of connected diagrams only. In order to construct the $\bar{H}$ diagrams we contract the Hamiltonian, H, with a number of T operators appearing in the e^T expansion. Since H contains at most four second quantized operators, it can be contracted to at most four T clusters (two in the case of the one-body component of H). If it is contracted to less, then the diagram can have some annihilation lines. Obviously, the diagram containing k annihilators, can be connected with at most $4 - k$ T clusters ($2 - k$ in the case of the one-body component). This means, e.g., that the contribution of $\bar{H}$ containing four annihilation lines represents just an element of H, and that containing three annihilation lines can be connected with 0 or 1 T cluster, etc. We can classify the $\bar{H}$ components into five different classes, having 0 to 4 annihilation lines:

$$\bar{H} = \bar{H}_0 + \bar{H}_1 + \bar{H}_2 + \bar{H}_3 + \bar{H}_4 \tag{8}$$

where the $\bar{H}_k$ represents all diagrams containing k annihilation lines. On the other hand, within each class we may separate $\bar{H}$ into contributions, distinguished by the superscript, engaging different numbers of excitations. Thus we may write:

$$\bar{H}_k = \sum_i \bar{H}_k^i \tag{9}$$

where i corresponds to the number of created quasi-particles, i.e., holes or true particles. In other words, i denotes the number of lines above the interaction line in an $\bar{H}$ diagram.

In general $\bar{H}$ is finite, but it can contain clusters up to N-fold excitations. Since the total number of particles in the system is constant, i.e., we do not allow for ionization processes, the summation over i in Eq. (9) runs over a subset of integers for which $i + k$ is even. The $(i + k)/2 = l$ in this context would correspond to the l-body component, $\bar{H}(l)$, of the effective hamiltonian. It follows immediately that to the 0-body part only $\bar{H}_0^0$ contributes, i.e.:

$$\bar{H}(0) = \bar{H}_0^0 \tag{10}$$

Analogously we have:

$$\bar{H}(1) = \bar{H}_0^2 + \bar{H}_1^1 + \bar{H}_2^0$$
$$\bar{H}(2) = \bar{H}_0^4 + \bar{H}_1^3 + \bar{H}_2^2 + \bar{H}_3^1 + \bar{H}_4^0 \tag{11}$$

and similar expressions for the higher-body components.

4. CC method with inclusion of single, double, triple and quadruple excitations

The inclusion of the higher rank equations into a given CC model is relatively straightforward from the conceptual point of view. Within the current model the wave function is represented as:

$$\psi = e^T \Phi \tag{12}$$

where $T = T_1 + T_2 + T_3 + T_4$ and T_m is defined in Eq. (3b).

The respective sets of equations are obtained by the projection of the Schroedinger equation

$$e^{-T} H e^T \Phi = E\Phi \tag{13}$$

on to the subsets of singly, doubly, triply and quadruply excited configurations, which lead to the following set of equations:

$$
\begin{aligned}
D_1 T_1 = (F_N &+ F_N T_1 + F_N T_2 + W_N T_1 + W_N T_2 + W_N T_3 \\
&+ F_N T_1^2/2 + W_N T_1^2/2 + W_N T_1 T_2 + W_N T_1^3/3!)_C
\end{aligned} \tag{14a}
$$

$$
\begin{aligned}
D_2 T_2 = (W_N &+ F_N T_2 + F_N T_3 + W_N T_1 + W_N T_2 + W_N T_3 + W_N T_4 \\
&+ F_N T_1 T_2 + W_N T_1^2/2 + W_N T_1 T_2 + W_N T_1 T_3 + W_N T_2^2/2 \\
&+ W_N T_1^3/3! + W_N T_1^2 T_2/2 + W_N T_1^4/4!)_C
\end{aligned} \tag{14b}
$$

$$
\begin{aligned}
D_3 T_3 = (F_N T_3 &+ F_N T_4 + W_N T_2 + W_N T_3 + W_N T_4 + F_N T_1 T_3 + F_N T_2^2/2 + W_N T_1 T_2 \\
&+ W_N T_1 T_3 + W_N T_1 T_4 + W_N T_2^2/2 + W_N T_2 T_3 + W_N T_1^2 T_2/2 \\
&+ W_N T_1 T_2^2/2 + W_N T_1^2 T_3/2 + W_N T_1^3 T_2/3!)_C
\end{aligned} \tag{14c}
$$

$$
\begin{aligned}
D_4 T_4 = (F_N T_4 &+ W_N T_3 + W_N T_4 + F_N T_1 T_4 + F_N T_2 T_3 + W_N T_1 T_3 + W_N T_3^2/2 \\
&+ W_N T_1 T_4 + W_N T_2^2/2 + W_N T_2 T_3 + W_N T_2 T_4 + W_N T_1^2 T_3/2 \\
&+ W_N T_1 T_2^2/2 + W_N T_1^2 T_4/2 + W_N T_2^3/3! + W_N T_1 T_2 T_3 \\
&+ W_N T_1^3 T_3/3! + W_N T_1^2 T_2^2/4)_C
\end{aligned} \tag{14d}
$$

where projection on the right of Eq. (14) by the Fermi vacuum $|0\rangle$ is understood, as is projection on the left by single (14a), double (14b), triple (14c) and quadruple excitations (14d), respectively. Also, the diagonal part of $F_N T_n$ has been taken to the left side of Eq. (14) in each case as $D_n T_n = (f_{ii} + f_{jj} + \cdots - f_{aa} - f_{bb} + \cdots)T_n$, for $i, j, \ldots$ occupied and $a, b, \ldots$ unoccupied in the reference state.
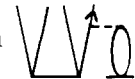
The standard procedure for derivation of the explicit CC equations, i.e., expressed in terms of individual amplitudes and integrals is to rewrite Eqs. (14a–14d) in diagrammatic form and then apply well-known rules [13] to translate them into algebraic language. We obtain for Eqs. (14a), (14b), (14c), and (14d) respectively 15, 38, 53, and 74 antisymmetrized diagrams. These diagrams are shown elsewhere [13, 11, 24], except for Eq. (14d) which are in Fig. 1, but in fact they are not really necessary here, since the same equations will be expressed in a much more compact, factorized form. In the case where we need a particular nonfactorized diagram for comparison purposes we will quote the respective diagram.

Fig. 1. All antisymmetrized diagrams that contribute to T_4 in the CCSDTQ equations
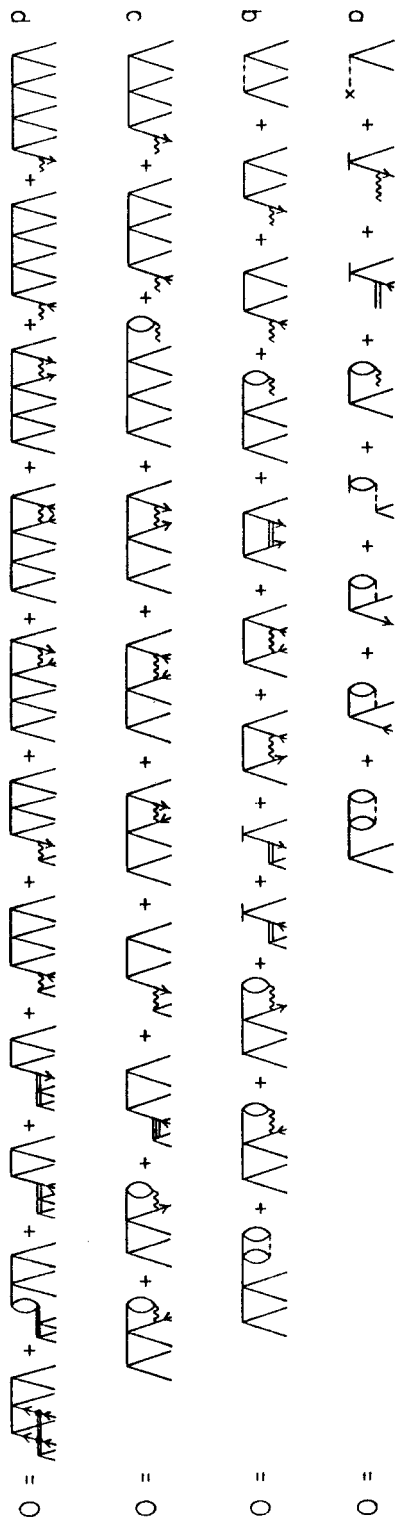
5. Factorization of the CCSDTQ equations

The diagrammatic equations corresponding to Eqs. (14a–14d) as shown in Fig. 1 for T_4 contain a very large number of terms. Programming them one by one is impractical; and the necessary computational effort would be unrealistic even in a situation where each of the diagrams is computed at modest cost. Obviously, each diagram is unique as a whole entity, many of them, though, are constructed of similar fragments which can be evaluated using the same program. The purpose of this section is to reformulate the coupled cluster equations in such a way that *all* the common pieces could be factored, computed only once, and then substituted into different places. This procedure is possible due to the fact that coupled cluster diagrams are in fact "denominator-less." By this we mean that the denominator is implicitly included in the vertex which avoids assigning denominators to each diagram like we do in the case of MBPT diagrams. This enables us to sum over all internal lines belonging to one T vertex independently of the other T vertices. This maneuver is applicable obviously only to nonlinear terms, i.e., to those in which an F_N or W_N vertex is connected with more than one T vertex. Our ultimate goal is to rewrite the CC equations in such a way that only *linear terms* with redefined vertices are retained in each equation. Thus in each nonlinear term we retain one t amplitude, usually (but not always) that corresponding to the highest excitation, whereas the others are absorbed in a generalized vertex. For instance, we may replace the diagram [diagram] with [diagram] where the new vertex [diagram] may be expressed graphically as:

$$[diagram] \quad = \quad [diagram]$$

   Although the original diagram, having three internal and four external lines, requires an $n^3 N^4$ step, after replacement, it requires two steps, one of $n^2 N^3$ and the other $n^2 N^2$ which is highly desirable, in fact, essential, computationally. This procedure is exploited to some degree in any computer implementation of the coupled cluster equations. However, the factorization of the CC diagrams has been introduced independently, and there has been less attempt to approach the problem globally in the context of a more elaborate coupled cluster method like CCSDTQ. In this section we are going to present the maximum possible factorization of the CCSDTQ equations. Total factorization means that *all the nonlinear terms should not explicitly appear in the final factorized equation.* In other words instead of the 15, 38, 53 diagrams shown in Ref. [13] plus the additional T_4 into T_2 and T_3 contributions and the 74 T_4 diagrams in Fig. 1, we obtain the 8, 12, 10, and 11 diagrams presented in Figs. 2a to 2d, respectively. These are expressed in algebraic form in Table 1, at the expense of the introduction of new dressed $\tilde{F}_N$ and $\tilde{W}_N$ vertices. The real computational advantage lies in the fact that (i) the newly introduced vertices are in most cases the same for all the equations and (ii) their evaluation is in most cases straightforward and suited to convenient supercomputer oriented matrix products.
   Furthermore, the introduced intermediates, presented in Fig. 3, are in most cases complete. For diagrams numbers 1 to 10, their form does not depend on the truncation of T. Hence, they will not change if we go beyond the SDTQ approximation. In the context of what has been said in Sect. 3 about the

S. A. Kucharski and R. J. Bartlett

Fig. 2. Diagramatic coupled cluster SDTQ equations with total factorization of nonlinear terms

Table 1. Coupled cluster equations for SDTQ model in algebraic from[a]

$$D_i^a t_i^a = f^{ai} + \chi_e^a t_i^e - \chi_m^{'i} t_m^a + \chi_{em} t_{mi}^{ea} + \tfrac{1}{2}\langle ma\|ei\rangle t_m^e + \tfrac{1}{2}\langle ma\|ef\rangle t_{mi}^{ef}$$
$$- \tfrac{1}{2}\langle mn\|ei\rangle t_{mn}^{ea} + \langle mn\|ef\rangle t_{mni}^{efa}$$

$$D_{ij}^{ab} t_{ij}^{ab} = \langle ab\|ij\rangle + P(ab)\chi_e^b t_{ij}^{ae} - P(ij)\chi_m^j t_{im}^{ab} + \chi_{em} t_{mij}^{eab} + \tfrac{1}{2}\chi_{ef}^{'ab} t_{ij}^{ef}$$
$$+ \tfrac{1}{2}\chi_{mn}^{ij} t_{mn}^{ab} - P(ab)(ij)\chi_{me}^{ib} t_{mj}^{ae} + P(ij)\chi_e^{'abj} t_i^e - P(ab)\chi_m^{njb} t_m^a$$
$$+ \tfrac{1}{2}P(ab)\chi_{fem}^a t_{mij}^{efb} - \tfrac{1}{2}P(ij)\chi_{nme}^i t_{mnj}^{eab} + \tfrac{1}{4}\langle mn\|ef\rangle t_{mnij}^{efab}$$

$$D_{ijk}^{abc} t_{ijk}^{abc} = P(c/ab)\chi_e^c t_{ijk}^{abe} - P(k/ij)\chi_m^k t_{ijm}^{abc} + \chi_{me} t_{mijk}^{eabc} + \tfrac{1}{2}P(c/ab)\chi_{ef}^{ab} t_{ijk}^{efc}$$
$$+ \tfrac{1}{2}P(k/ij)\chi_{mn}^{ij} t_{mnk}^{abc} - P(i/jk)(b/ac)\chi_{me}^{ib} t_{mjk}^{aec} + P(k/ij)(a/bc)\chi_e^{bck} t_{ij}^{ae}$$
$$- P(i/jk)(c/ab)\chi_m^{njkc} t_{im}^{ab} + \tfrac{1}{2}P(a/bc)\chi_{efm}^a t_{mijk}^{efbc} - \tfrac{1}{2}P(i/jk)\chi_{mne}^i t_{mnjk}^{eabc}$$

$$D_{ijkl}^{abcd} t_{ijkl}^{abcd} = P(d/abc)\chi_e^d t_{ijkl}^{abce} - P(l/ijk)\chi_m^l t_{ijkm}^{abcd} + \tfrac{1}{2}P(ab/cd)\chi_{ef}^{ab} t_{ijkl}^{efcd}$$
$$+ \tfrac{1}{2}P(ij/kl)t_{mnkl}^{abcd} - P(i/jkl)(b/acd)\chi_{me}^{ib} t_{mjkl}^{aecd} + P(ab/cd)(ijk/l)\chi_e^{cdl} t_{ijk}^{abe}$$
$$- P(abc/d)(ij/kl)\chi_m^{kld} t_{ijm}^{abc} + P(a/bcd)(ij/kl)\chi_e^{'bckdl} t_{ij}^{ae} - P(ab/cd)(i/jkl)$$
$$\times \chi_m^{'jckdl} t_{im}^{ab} - P(ab/cd)(ij/kl)\chi_{me}^{'kcld} t_{ijm}^{abe} + \tfrac{1}{2}P(abc/d)(i/jkl)\chi_{mn}^{ijkdl} t_{imn}^{abc}$$

[a] Permutation symbols are the same as in Refs. [7, 24]. $P(ab/cd)$ (ijk/l) means that in addition to the identity permutation, all possible products involving permutations of a and b; c and d, and ij and k are allowed

structure of the effective hamiltonian, it is not very difficult to observe that they correspond to different $\bar{H}_i^k$ of the $\bar{H}$ operator. In Fig. 3 we identify diagram 1 as $\bar{H}_2^0$, diagrams 2 and 3 as $\bar{H}_1^1$; diagram 6 as $\bar{H}_2^2$ etc. Thus the one-body part of $\bar{H}$ may be expressed as the sum of the diagrams:

$$\bar{H}(1) = I1 + I2 + I3 \tag{15}$$

where I_k corresponds to intermediate diagram no. k in Fig. 3. This means that when using this total factorization scheme we have obtained as a byproduct an expansion for the low rank components of $\bar{H}$. Now we will write the CC equations within a given model in terms of $\bar{H}$ type intermediates.

In the T_1 equation we have seven nonlinear diagrams corresponding to four nonlinear terms in Eq. (14a). They are all accounted for by introducing one-body intermediates, numbered 1, 2, and 3a in Fig. 3. The first two vertices, i.e.,

and , are the same for all the equations considered, i.e., they are complete, the third one, I3a, , is incomplete and must be augmented by one more diagram when going to higher (than one) rank equations. Using that vertex in its complete form, i.e., I3 instead of I3a, in the T_1 equation would result in overcounting some diagrams. Now using the $\bar{H}$ based intermediates we may write the T_1 equation corresponding to Eq. (14a) as:

$$\langle \Phi_i^a \| [H_0, T] | \Phi \rangle = \langle \Phi_i^a \| [\bar{H}'(1) + W_N, T] | \Phi \rangle \tag{16}$$
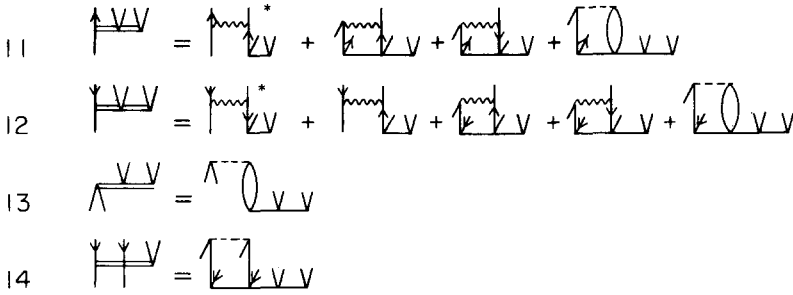
Fig. 3. The intermediates introduced in CCSDTQ model with total factorization of nonlinear terms

where the prime denotes that $\bar{H}$ is not complete, since it includes the $I3a$ $(\chi_j^{'i})$ contribution instead of the $I3$ (χ_j^i) one. The commutator ensures that all unlinked or disconnected diagrams are eliminated. All the intermediates used in the T_1 equation are computed with no higher than an n^2N^3 scale factor. The same factor occurs for all the diagrams occurring in the factorized T_1 equation, see Fig. 1a, except for the last one which requires an n^2N^4 scheme.

In Fig. 1b the factorized form for the T_2 equation is shown. Out of twelve diagrams contributing to this equation, two, i.e., the first and last one, are in their original forms, i.e., they engage nondressed vertices: the first one because this is just a W_N operator and the last one because we cannot dress the W_N vertex containing exclusively annihilation operators. All the 38 original diagrams corresponding to Eq. (14b) are reproduced when we replace the dressed vertices in Fig. 2b by their diagrammatic components as given in Fig. 3. In addition to $\bar{H}(1)$ we introduce the $\bar{H}(2)$ component of $\bar{H}$ as:

$$\bar{H}(2) = I4 + I5 + I6 + I7 + I8 + I9 + I10 \qquad (17)$$

Equivalently, we could express $\bar{H}(2)$ in terms of algebraic quantities defined in Table 2, Eqs. (4–10). Similarly as in the case of the T_1 equation, in order to prevent overcounting, some of the newly defined vertices – three in this case:
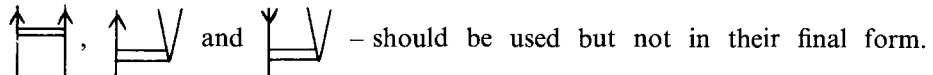
 , and – should be used but not in their final form.
The T_2 equation may now be expressed as

$$\langle \Phi_{ij}^{ab} |[H_0, T]|\Phi\rangle = \langle \Phi_{ij}^{ab} |[H(1) + \bar{H}'(2), T]|\Phi\rangle \qquad (18)$$

where again the prime refers to the situation that not all of the components of $\bar{H}$ are in their complete form. All the intermediates occurring in the T_2 equation are obtained with n^2N^4 and lower scaling factors. The same factor occurs in the case of diagrams contributing to the T_2 equation, in Fig. 2b, with the exception of the last three. The latter represent contributions from T_3 and T_4 cluster operators and are computed via n^3N^4 and n^4N^4 schemes, respectively.

The third type of equation, i.e., T_3, is presented in a factorized form in Fig. 2c. All of the new $\tilde{W}_N$ vertices are used in their full form except for that carrying number $I10$ in Fig. 3,

$$\langle \Phi_{ijk}^{abc} |[H_0, T]|\Phi\rangle = \langle \Phi_{ijk}^{abc} |[\bar{H}(1+)\bar{H}''(2), T]|\Phi\rangle \qquad (19)$$

where the double prime means that the $I10$ diagram is replaced with $I10a$. Again most of the intermediates are computed with n^2N^4 and lower factors.

Table 2. Algebraic expression for the intermediates defined in Fig. 2

$$\chi_{ia} = f_{ia} + \langle im \| ae \rangle t_m^e \tag{1}$$

$$\chi_b^a = f_b^a + \langle am \| be \rangle t_m^e - \chi_{mb} t_m^a - \tfrac{1}{2} \langle mn \| eb \rangle t_{mn}^{ea} \tag{2}$$

$$\chi_i^j = \chi_i'^j + \chi_{ie} t_j^e \tag{3}$$

$$\chi_i'^j = f_i^j + \langle im \| je \rangle t_m^e + \tfrac{1}{2} \langle mi \| ef \rangle t_{mj}^{ef} \tag{3a}$$

$$\chi_{bci}^a = \chi_{bci}'^a - \tfrac{1}{2} \langle mi \| bc \rangle t_m^a \tag{4}$$

$$\chi_{bci}'^a = \langle ai \| bc \rangle - \tfrac{1}{2} \langle mi \| bc \rangle t_m^a \tag{4a}$$

$$\chi_{ija}^k = \chi_{ija}'^k + \tfrac{1}{2} \langle ij \| ea \rangle t_k^e \tag{5}$$

$$\chi_{ijk}'^k = \langle ij \| ka \rangle + \tfrac{1}{2} \langle ij \| ea \rangle t_k^e \tag{5a}$$

$$\chi_{cd}^{ab} = \chi_{cd}'^{ab} + \tfrac{1}{2} \langle mn \| cd \rangle t_{mn}^{ab} \tag{6}$$

$$\chi_{cd}'^{ab} = \langle ab \| cd \rangle + P(ab) \chi_{cdm}'^a t_m^b \tag{6a}$$

$$\chi_{ij}^{kl} = \langle ij \| kl \rangle + P(kl) \chi_{ije}'^k t_l^e + \tfrac{1}{2} \langle ij \| ef \rangle t_{kl}^{ef} \tag{7}$$

$$\chi_{ib}^{ja} = \chi_{ib}'^{ja} + \langle im \| eb \rangle t_{jm}^{ea} \tag{8}$$

$$\chi_{ib}'^{ja} = \langle ia \| jb \rangle - \langle im \| jb \rangle t_m^a + \chi_{bei}^a t_i^e \tag{8a}$$

$$\chi_{ib}''^{ja} = \langle ia \| jb \rangle - \langle im \| jb \rangle t_m^a + \chi_{bei}'^a t_i^e \tag{8b}$$

$$\chi_c^{abi} = \chi_c'^{abi} + \langle ab \| ce \rangle t_i^e - P(ab) \chi_{mc}'^{ia} t_m^b - \chi_{mc} t_{mi}^{ab}$$
$$\qquad - P(ab) \chi_{fcm}^b t_{mi}^{af} + \chi_{nmc}^i t_{mn}^{ab} - \tfrac{1}{2} \langle mn \| ce \rangle t_{mni}^{aeb} \tag{9}$$

$$\chi_c'^{abi} = \langle ab \| ci \rangle + \tfrac{1}{2} \langle ab \| ce \rangle t_i^e - P(ab) \chi_{mc}''^{ia} t_m^b \tag{9a}$$

$$\chi_i^{jka} = \chi_i''^{jka} + \chi_{ie} t_{jk}^{ea} \tag{10}$$

$$\chi_i''^{jka} = \chi_i'^{jka} - \tfrac{1}{2} \langle im \| jk \rangle t_m^a + P(jk) \chi_{ie}'^{ja} t_k^e$$
$$\qquad + \tfrac{1}{2} \chi_{fei}^a t_{jk}^{ef} - P(jk) \chi_{mie}^k t_{jm}^{ea} + \tfrac{1}{2} \langle im \| ef \rangle t_{jmk}^{efa} \tag{10a}$$

$$\chi_i'^{jka} = \langle ia \| jk \rangle - \tfrac{1}{2} \langle im \| jk \rangle t_m^a \tag{10b}$$

$$\chi_d'^{abicj} = \tfrac{1}{2} P(c/ab) \chi_{de}^{ab} t_{ij}^{ec} - \chi_{edm}^b P(b/ac) t_{mij}^{aec} + P(ij) \chi_{nmd}^i t_{mnj}^{abc} - \langle mn \| de \rangle t_{mnij}^{aebc} \tag{11}$$

$$\chi_i'^{jakbl} = -\tfrac{1}{2} P(l/jk) \chi_{im}^{jk} t_{ml}^{ab} + P(ab)(j/kl) \chi_{ie}^{ja} t_{kl}^{eb} -$$
$$\qquad + P(ab) \chi_{fei}^a t_{jkl}^{efb} - P(k/jl) \chi_{mie}^k t_{jml}^{eab} + \langle im \| ef \rangle t_{jmkl}^{efab} \tag{12}$$

$$\chi_{ib}'^{jack} = - \langle im \| eb \rangle t_{jmk}^{eac} \tag{13}$$

$$\chi_{ij}'^{klai} = \langle ij \| ef \rangle t_{kli}^{efc} \tag{14}$$

Only two of them require higher, i.e., an $n^3 N^4$ scheme and those are displayed as the last contributions to the wiggly vertices in Fig. 3, diagrams 9 and 10.

More demanding computationally are the diagrams present in the factorized T_3 equation, see Fig. 2c. As in the previous cases only diagrams formally linear in T occur and in most of them these are T_3 vertices. The presence of T_3 amplitudes usually invokes a higher scaling factor and this is the case here. The computationally simplest diagrams correspond to an $n^3 N^4$ scheme, and are those involving the T_2 vertex or T_3 combined with a one-body vertex. The others like those combining a T_3 amplitude with a two-body vertex or a T_4 amplitude with a one-body vertex are of $n^4 N^4$ dependence. Finally the toughest ones are those

expressing the T_4 to T_3 contribution via a two-body vertex which scales as n^4N^5. Bearing in mind that most of the intermediates have already been computed for lower rank equations the real effort required to code the T_3 equation is programming the diagrams listed in Fig. 2c. From the programmer point of view this is not that demanding a task once the $\tilde{W}_N$ vertices are available. Moreover, we observe that in such a formulation of the CC method in which the real computational effort is expended when computing the linear terms, the inclusion of the nonlinear terms has a negligible effect on the cost of computations and also is connected with minimum additional programming effort.

The same situation to a certain degree is repeated in the T_4 equation. The T_4 equation, presented in factorized form in Fig. 2d contains eleven terms and for their evaluation we need eleven dressed vertices. Seven of them: $I2$–$I6$, $I9$, and $I10$ are those already defined for lower rank CC equations, and the only modification is that we used $I10$ instead of $I10a$, but this is a matter of inclusion of only one more diagram which has an n^2N^3 scaling factor. This means that in the current equation we will use complete one- and two-body components of $\bar{H}$. In addition we introduce four additional intermediates, $I11$ to $I14$, as components of $\bar{H}(3)$. Now the T_4 equation may be written as:

$$\langle \Phi_{ijkl}^{abcd} | [H_0, T] | \Phi \rangle = \langle \Phi_{ijkl}^{abcd} | [\bar{H}(1) + \bar{H}(2) + \bar{H}'(3), T] | \Phi \rangle \tag{20}$$

where the three-body part of $\bar{H}$ is expressed as:

$$\bar{H}'(3) = I11 + I12 + I13 + I14 \tag{21}$$

Thus the new vertex, no. 11 in Fig. 3, is obtained as a contribution from nine intermediate diagrams. That in itself would be a difficult problem, however, we may facilitate it by using in its evaluation the other wiggly vertices defined previously. Due to that the number of contributions to be accounted for is reduced to four, see Fig. 3. Analogously, the wiggly vertex no. 12 in Fig. 3, being a sum of fourteen dashed-vertex diagrams, can be computed as a sum of five intermediates with previously defined vertices. This procedure for using the lower rank intermediates in the evaluation of their higher rank counterparts which we call the Recursive Generation of Intermediates (RGI), is a beneficial characteristic of the present approach and brings about a remarkable reduction both in the programmer's and the computer's effort. The two wiggly vertices under consideration require for their evaluation much more time than all the previous ones. The intermediates contributing to vertex no. 11 are computed within an $n^3N^4(1)$, $n^4N^4(2)$, and $n^4N^5(1)$ scheme, where the numbers in parenthesis refer to the number of intermediates. Similarly, for the vertex no. 12 we have: $n^3N^4(2)$, $n^4N^4(2)$, $n^4N^5(1)$. The last two vertices in Fig. 2 represent one intermediate in each case and they are evaluated with an n^4N^4 dependence. Having created the necessary intermediates we may turn to the evaluation of the diagrams contributing to the T_4 equation, see Fig. 2d. Out of eleven diagrams six represent an n^4N^5 problem and the remaining five – an n^4N^6 problem.

6. Vectorization of the coupled cluster code

In order to fully exploit the currently existing computational facilities one needs to formulate the computational method in such a way that it could be easily

vectorized. In other words, we may benefit from vector architecture or array processors by rewriting the algorithm in terms of matrix multiplications. It is straightforward to see that the factorization of the coupled cluster equations introduced in the previous section is ideally suited for vectorization. This is due to the fact that each diagrammatic term occurring either in the expression for intermediates presented in Fig. 3 or for the factorized coupled cluster equations in Fig. 2, is composed of two vertices only: the (modified) interaction vertex $\tilde{F}_N$ or $\tilde{W}_N$ and the cluster vertex T. Hence each diagrammatic contribution is represented by a product of two quantities, each of them being a multidimensional array. It is obvious that this may be treated as a product of two matrices. Since this can be done for all diagrams appearing in Figs. 2 and 3, the full vectorization within the present formalism is easy to achieve.

Let us investigate the process of vectorization of the coupled cluster code using several examples. We begin with the simple diagram expressing a contribution into the t_i^a amplitude from the T_1 cluster via the one-body potential. This is expressed diagrammatically as $\vcenter{\hbox{\includegraphics{diagram}}}$ which may be written algebraically as:

$$t_i^a = \sum_e f_{ae} o_i^e \tag{22}$$

where the t and o symbols refer to the new and old t amplitudes, respectively. It is obvious that Eq. (22) may be considered as a product of two matrices: F and O_1:

$$T1(A, I) = \sum_E F(A, E) * O1(E, I) \tag{23}$$

where the meaning of symbols is obvious. Using matrix symbols:

$$T1 = FP * O1 \tag{24}$$

where FP denotes a matrix of one-body particle–particle intermediates. We assume that the general matrix multiplication routine called MATMUL works in such a way that the product of two matrices A and B:

$$C = A * B \tag{25}$$

of dimensions $A(NA, M)$ and $B(M, NB)$ gives matrix C of dimension $C(NA, NB)$ as

$$MATMUL(A, B, C, NA, NB, M) \tag{26}$$

Using the above procedure we may express Eqs. (22–24) in terms of the MATMUL routine as:

$$MATMUL(FP, O1, T1, NP, NH, NP) \tag{27}$$

where NH, NP refer to the number of hole and particle (occupied and virtual) levels in the system, respectively.
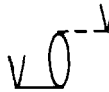
Using the same scheme we may express in terms of matrix multiplication a contribution coming from the diagram $\vcenter{\hbox{\includegraphics{diagram}}}$ as:

$$T1(A, I) = \sum_M O1(A, M) * FH(M, I) \tag{28}$$

or using the MATMUL routine as:

$$MATMUL(O1, FH, T1, NP, NH, NH) \qquad (29)$$

A more complicated situation occurs for cases involving double and higher excitation clusters as well as two-body intermediates. In these cases we encounter higher than two-dimensional arrays. Hence the first step will be to reorganize them into two-dimensional ones by appropriate mapping of the indices. We will analyze this situation for the example of the diagram with the corresponding algebraic expression:

$$t_{ij}^{ab} = \sum_{me} o_{im}^{ae} \langle mb | ej \rangle \qquad (30)$$

Each of the entities in the last formula must be expressed as a two-dimensional array and by the following transformation of the indices: $i, a \rightarrow K; j, b \rightarrow L$; and $m, e \rightarrow P$ we obtain the mapping $t_{ij}^{ab} \rightarrow T2(K, L)$; $o_{im}^{ae} \rightarrow O2(K, P)$; and $\langle mb | ei \rangle \rightarrow V(P, L)$. Now the formula (30) can be written as:

$$T2(K, L) = \sum_{P} O2(K, P) * V(P, L) \qquad (31)$$

where K, L, and P run over $NH * NP$ levels. Using the MATMUL routine the last expression may be replaced with:

$$MATMUL(O2, V, T2, NHP, NHP, NHP) \qquad (32)$$

where $NHP = NH * NP$.

A closer examination of the above procedure tells us that the reorganization of the four-dimensional arrays into two-dimensional ones is not necessary provided a correct ordering of the involved indices is arranged. If the matrices corresponding to the amplitudes t_{ij}^{ab} are arranged as $T2(I, A, J, B)$, o_{im}^{ae} as $O2(I, A, M, E)$ and the integrals $\langle mb | ej \rangle$ are stored as $V(M, E, J, B)$ then the operation expressed in Eq. (32) still provides the correct contribution to the amplitude t_{ij}^{ab}. An analogous situation occurs for other diagrams. Let us consider as a next example a contribution to the intermediate coming from the diagram according to the formula:

$$VHPP(I, A, B, C) = \sum_{m} VHP(I, A, B, M) * T1(M, C) \qquad (33)$$

Using the MATMUL routine the last formula can be written as:

$$MATMUL(VHP, T1, VHPP, NHPP, NP, NH) \qquad (34)$$

where $NHPP = NH * NP * NP$.

We note that the t_i^a amplitudes occurring in Eq. (33, 34) are rearranged differently than those employed in Eqs. (27) and (29), since in the former the first index runs over hole levels whereas the latter runs over particle ones. We could possibly exchange the order of matrices in Eq. (34) to retain the structure of the $T1$ array; however, this would affect the order of indices in the VHHP intermediates. Thus in order to express a given contribution in terms

of a matrix product we must be aware of the fact that in many cases the matrices have to be transposed. This is a trivial procedure for the case of a two-dimensional square matrix. For the multidimensional array exchanging a pair or more of indices still can be easily handled on condition that the involved indices belong to the dimensions of the same length. It should be noted that the transposition step involves only one matrix at a time, be it amplitudes or an intermediate matrix, and because of that this step is usually of a much lower n scheme than the actual diagrammatic contribution which is a product of two matrices. It should be mentioned that some computers are equipped with efficient SCATTER/GATHER capabilities exploited in matrix multiplication which allows avoiding in most cases transposition of the involved matrices [25].

On the basis of the above examples we may now give general rules stating how to express a contribution from a given diagram directly in terms of a MATMUL subroutine.

Let us consider a general diagrammatic contribution to the t amplitude expressed diagrammatically as:

$$
\bigvee\!\ldots\!\bigvee \;=\; \bigvee\!\ldots\!\bigcap^{\ldots\vee} \tag{35}
$$

where the l.h.s. vertex and lower r.h.s. vertex corresponds to general new and old t amplitudes, T and O, respectively, whereas the upper vertex represents a graphical picture of the general intermediate $\tilde{W}$. We assume that all the lines attached to the intermediate vertex from below are connected with the O vertex and they become internal lines, i.e., those over which the actual summation is performed. On the other hand, all the lines connected to the intermediate from the top as well as the remaining lines in the lower (i.e. O) vertex constitute the open lines and their number exactly matches the total number of lines in the l.h.s. vertex.

The contribution from the general diagram presented above may be expressed with the help of the MATMUL routine as:

$$
MATMUL(O, V, T, NET, NEV, NI) \tag{36}
$$

or as

$$
MATMUL(V, O, T, NEV, NET, NI) \tag{37}
$$

where

$$
NET = LPET * NP * LHET * NH
$$

$$
NEV = LPEV * NP * LHEV * NH
$$

$$
NI = LPIT * NP * LHIT * NH
$$

and $LPET$ ($LHET$), $LPEV$ ($LHEV$) denote a number of external particle (hole) lines connected with O and V vertices, respectively and $LPIT$ ($LHIT$) refers to the number of internal particle (hole) lines.

Each of the two expressions given in Eqs. (36, 37) refer to the different situations: Eq. (36) corresponds to the product $T = O * V$ whereas the other one, Eq. (37), represents the product $T = V * O$. Which of the two expressions will be actually chosen depends on the current order of indices.

For the case represented by Eq. (36) indices must appear in the following order:

T vertex – labels on external lines, labels on internal lines

V vertex – labels on internal lines, labels on external lines

O vertex – labels on lines corresponding to those on the T vertex; labels on lines corresponding to those on the V vertex.

If the given contribution is evaluated according to Eq. (37) the order of two groups of labels on each vertex is reversed. It must be stressed that the order of labels on internal lines on both vertices must be matching. Similarly, the order of labels on the T vertex strictly follows the order of open lines on the O and V vertices.

The following example will help to clarify the above rules. Let us evaluate the contribution to the t_{ij}^{ab} amplitude coming from the $W_N T_3$ term via the diagram
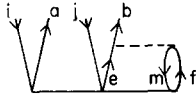
 . The routine MATMUL will be called with the following
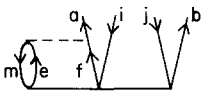
parameters:

$$MATMUL(O3, VHPP, T2, NET, NEV, NI) \qquad (38)$$

where $NET = NH * NH * NP$; $NEV = NP$; $NI = NH * NP * NP$. The order of the indices within each of the involved arrays, i.e. $O3$, $VHPP$ and $T2$ can be, e.g. as follows: $O3(I, J, A, E, F, M)$, $VHPP(E, F, M, B)$, $T2(I, J, A, B)$.

We may change the order within the first three indices of $O3$ (accompanied by the matching change within the first three indices of $T2$) as well as the order within the last three indices of $O3$ (accompanied by the matching reordering of the first three indices within the VHHP intermediate).

We may as well invoke the MATMUL routine according to the pattern of Eq. (39). In this case we have to relabel the lines in the diagram
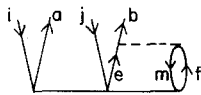
 as follows: . The respective routine will

be now called:

$$MATMUL(VHPP, O3, T2, NEV, NET, NI) \qquad (39)$$

where the last three parameters have the same values as in Eq. (38). The order of indices within each of the arrays is as follows:

$$VHPP(A, E, F, M), O3(E, F, M, B, I, J), T2(A, B, I, J)$$

Similarly as before we may change the order within certain groups of indices on condition that the changes will be identical within each pair of the concerned arrays.

Which of the two possible calls of MATMUL routine will actually be performed depends on the current structure of the arrays. Generally, we will choose that option which requires less index reordering in the matrices to be multiplied.

The last examples illustrate clearly the use of general rules which allow for the mnemonic assignment of the MATMUL routine equipped with appropriate parameters for each coupled cluster diagram.

So far we have not paid attention to such factors connected with each of the spin-adapted Goldstone diagrams that derive from the antisymmetrized diagrams, such as sign, coefficients due to presence of the closed loops in the diagrams (2^l, l = number of loops) and coefficients due to the presence of a symmetry plane (1/2). In fact, these coefficients do not affect a general vectorization scheme since they can be accounted for in a different way. For instance, in the diagram evaluated via Eq. (38) a factor of two must be included due to the presence of the closed loop. To account for it we need to multiply one of the involved arrays by two before invoking the MATMUL routine. Usually we do this for whichever of the two matrices is smaller. In the present case this will be the VHPP matrix. This is a very fast step compared to the matrix multiplication: $NH * NP^3$ versus $NH^3 * NP^4$. If the same VHPP array is to be used in the evaluation of the next diagram which come with a different factor, we must remultiply VHPP by a suitable coefficient. We may still reduce the time needed for preparing the arrays for the actual evaluation of the diagram (i.e., premultiplication by some coefficient, multidimensional transposition) by simply collecting together all those diagrams which require the requisite type of input arrays.

For convenience, we have assumed the situation that all the arrays involved in the evaluation of the given diagram can be kept in the physical memory of the computer. Of course, this is unrealistic for CC models involving T_3 and T_4 clusters or for large basis sets, where the integrals, particularly the 4-virtual orbital case $\langle ab | cd \rangle$, are excessive. Consequently, despite the availability of computers with large core memory, IO is inevitable for large basis examples and must be handled intelligently to be balanced appropriately against the CPU time. Obviously, the way one handles this problem is by restricting some indices while processing others. For the $n_0^2 n_{virt}^4$ step:

$$ t_{ij}^{ab} = \sum_{c > d} \langle ab \| cd \rangle t_{ij}^{cd} $$

we will typically sort integrals to read from external storage all cd for a given ab choice, and perhaps with a one (or several) choices of i, j as required by memory constraints.

It is obvious from the above discussion that if we retain the proposed transparent structure of the CC equations and code them using RGI strategy we can easily express the entire complicated program in terms of one elementary operation: the matrix multiplication. Then we may focus attention on all the steps involving larger matrices which become a bottleneck for the efficiency of the program while leaving the other steps unaffected. The construction of the whole program from independent pieces is in practice a very useful property. The further addition of Abelian symmetry to an intermediate driven structure for CCSD has paid enormous dividends in efficiency [26].

7. Conclusions

We have presented a very compact form of the SDTQ coupled cluster equations. The final computational equations require only terms that are formally linear, since the nonlinear ones are included by a suitable definition of intermediates. The latter are calculated in a recursive manner which significantly reduces

the number of terms to be programmed. All the terms occurring either in the evaluation of the intermediates or in calculating a contribution to the T amplitude are computed as a product of two quantities: the $\tilde{F}_N$ and $\tilde{W}_N$ vertex and a T amplitude. This means that the entire computational scheme is composed of steps computed as a product of two (super) matrices. This feature of the current approach is valuable from the point of view of possible vectorization of the program. In addition, the whole construction of the method is very straightforward and can be easily implemented. Full CCSDTQ results are reported elsewhere [27]. The further refinement of the program is reduced to work on large matrix multiplication routines.

References

1. Čížek J (1966) J Chem Phys 45:4256; (1969) Adv Chem Phys 14:15
2. Coester F, Kümmel H (1960) Nucl Phys 17:477; Bartlett RJ (1989) J Phys Chem 93:1697; (1981) Ann Rev Phys Chem 32:359
3. Paldus J, Cizek J, Shavitt I (1974) Phys Rev A5:50
4. Bartlett RJ, Purvis GD (1978) Int J Quantum Chem 14:561; (1980) Physica Scripta 21:255
5. Pople JA, Krishnan R, Schlegel HB, Binkley JS (1978) Int J Quantum Chem 14:545
6. Purvis GD, Bartlett RJ (1981) J Chem Phys 75:1284
7. Lee YS, Kucharski SA, Bartlett RJ (1984) J Chem Phys 84:5906
8. Urban M, Noga J, Cole SJ, Bartlett RJ (1986) J Chem Phys 83:4041
9. Noga J, Bartlett RJ, Urban M (1987) Chem Phys Lett 134:126
10. Noga J, Bartlett RJ (1987) J Chem Phys 86:7041; (1988) ibid 89:3401; Scuseria G, Schaefer III HF (1988) Chem Phys Lett 152:382; Watts JD, Bartlett RJ (1990) J Chem Phys 93:6104
11. Kucharski SA, Bartlett RJ (1989) Chem Phys Lett 158:550
12. Bartlett RJ, Watts JD, Kucharski SA, Noga J (1990) Chem Phys Lett 165:513
13. Kucharski SA, Bartlett RJ (1986) Adv Quantum Chem 18:281
14. Lindgren I, Mukherjee D (1987) Phys Rep 151:93; Stolarczyk LZ, Monkhorst HJ (1986) Phys Rev A32:725; Paldus J (1983) in: Löwdin and Pullman (eds) New horizons of quantum chemistry. Reidel, Dordrecht, p 31; Meissner L, Bartlett RJ (1989) J Chem Phys 91:4800
15. Monkhorst HJ (1977) Int J Quantum Chem Symp 11:421; Sekino H, Bartlett RJ (1984) Int J Quantum Chem Symp 18:255
16. Salter EA, Trucks GW, Bartlett RJ (1989) J Chem Phys 90:1952; Bartlett RJ (1986) in: Jørgensen and Simons (eds) Geometric derivatives of energy surfaces and molecular properties. Reidel, Dordrecht, The Netherlands, p 35
17. Emrich K (1981) Nucl Phys A351:397; Nakatsuji H, Hirao K (1978) J Chem Phys 68:2053; (1978) ibid 69:4548
18. Geertsen J, Rittby M, Bartlett RJ (1989) Chem Phys Lett 164:57
19. Takahashi M, Paldus J (1986) J Chem Phys 85:1486
20. Lindgren I (1986) Int J Quantum Chem 20:409; Mukherjee D (1986) Chem Phys Lett 125:207
21. Haque A, Kaldor U (1985) Chem Phys Lett 117:347; (1985) 120:261; Kaldor U (1986) Int J Quantum Chem S20:409
22. Pal S, Rittby M, Bartlett RJ, Sinha D, Mukherjee D (1987) Chem Phys Lett 137:273; (1988) J Chem Phys 88:4357; Pal S, Rittby M, Bartlett RJ (1989) Chem Phys Lett 160:212
23. Rittby M, Pal S, Bartlett RJ (1989) J Chem Phys 90:3214
24. Bartlett RJ, Kucharski SA (to be published) Comp Phys Rep
25. Bauschlicher Jr CW, Partridge H (1987) J Compt Chem 8:636
26. Stanton JF, Gauss J, Watts JD, Bartlett RJ (1991) J Chem Phys 94:4334
27. Kucharski SA, Bartlett RJ (to be published)